# REAL TIME OPTIMAL IMPLEMENTATION OF STABILIZING CONTROLLER FOR INVERTED PENDULUM

**M. Idi[1,2], N. M. Tahir[1*], A. G. Ibrahim[1,2]**

[1]Department of Mechatronics and System Engineering, Abubakar Tafawa Balewa University (ATBU) Bauchi, Nigeria.
[2]Faculty of Engineering and Built Environment Glasgow Caledonian University, Scotland, UK.

Article History: Received 29.8.2017; Revised 13.8.2018; Accepted 26.12.2018

***ABSTRACT***

*This paper present real time control of an inverted pendulum. The system is inherently unstable and multivariable. It is mostly used in laboratories to study, verify and validate new control ideas. The dynamic model of the system was derived based on Lagrange approach and it was linearized. Linear Quadratic Regulator (LQR) controller was designed to stabilize the system in an upright position. The robustness of the control algorithm was tested based on disturbance rejection. Simulation and experimental results showed a good performance was achieved and the controller is robust to external disturbances.*

***KEYWORDS****: Nonlinear; LQR; inverted pendulum;disturbance rejection; Lagrange*

## 1.0 INTRODUCTION

An inverted pendulum is a multivariable, an under-actuated, nonlinear, and unstable system, (Mus & Tovornik, 2006), (Riachy et al, 2007), (Jerome et al, 2013). Due to these dynamics, it is mostly used by researchers to investigate the control algorithms. Modelling and control of the nonlinear inverted pendulum system is one of the major areas of research with lots of potentials in the field of robotics and automation. Various researchers have proposed different control algorithms and techniques for swing up, tracking and stabilization of an inverted pendulum.

Balancing an inverted pendulum mobile robot using LQG and LQR has been proposed by Hauser and Saccon (2005), and their performances were compared. Modelling and a predictive controller based on the nonlinear model of the

* Corresponding author. Email: nuratahir85@gmail.com

system have been presented in Chalupa (2008). Similarly, Prasad (2014), Singh and Yadav (2012) and Gupta (2014) compared the stabilization and swing up control performances of LQR and PID controllers for an inverted pendulum. The stabilization control of an inverted pendulum using Pole Placement and LQR has been presented in Kumar et al (2012), a comparison of the control algorithms has also been presented.

Furthermore, an MODE-based optimized LQR developed in Tijani (2013) shows a superior performance. Singh et al (2014) used a modified PSO based PID sliding mode for swing up and stabilization control of an inverted pendulum. In addition, Chakraborty et al (2013) investigated the optimization of PID controller using Genetic Algorithm. A dynamic modelling and optimal control of wheel inverted pendulum were proposed in Shamsudin et al (2013) using an optimally tuned partial-state PID. Swing up and stabilization of double inverted pendulum using LQR and LQR based fuzzy was proposed in Bhangal (2013), and their performances were analyzed and compared. An intelligent control algorithm has also been proposed in A-hadithi (2012) and implemented for swing up and stabilization of a double inverted pendulum system.

The combinations of intelligent and conventional control have shown good performances and robustness of the control algorithms. An Adaptive Neural Network for motion control of a wheeled, inverted pendulum has also been presented in Yang et al (2014). In Chalupa and Bobal (2008), Model Predictive Controller has been proposed. A novel PSO based Sliding Mode Control for stabilization of an inverted pendulum was presented by Singh et al (2014). In Brisilla and Sankaranarayanan (2015), a stabilization of an inverted pendulum using a nonlinear control algorithm has been presented.

However, to implement a simple control algorithm and obtained stability under external disturbances is a big challenging task. Thus, using LQR the stability and control of all system poles are guaranteed. This paper proposed LQR for real time stabilization of an inverted pendulum under wind disturbances of magnitude of 0.2 N. Time response specification and level of disturbances rejections were used as the performance index of the control algorithms.

## 2.0 SYSTEM DESCRIPTION

In this part, the inverted pendulum dynamics is presented.

### 2.1 An Inverted Pendulum System

In this work, the laboratory scale feedback digital pendulum system version 33-000-V73 was used. The system consists of the following parts; the cart, two pendulums, a rail, and a D.C motor. The pendulum is hinged at the center of the cart in a manner that they can rotate freely for 360°. The cart can move freely horizontally on the rail with the aid of the D.C motor. The mechanical system is as shown in Figure1.

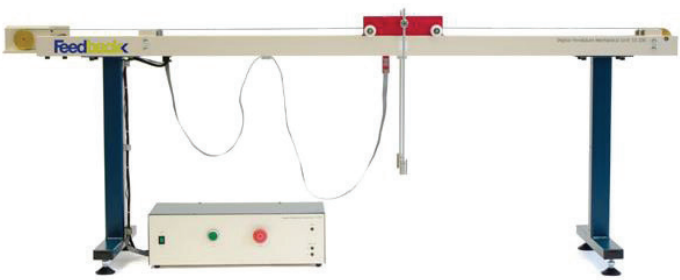


Figure 1. The laboratory-based Inverted Pendulum

When the pendulum is in the vertical position, the system is unstable and when the pendulum is in a downward position, the system is completely stable. The pendulum is completely unstable for small deviations from the equilibrium position. Figure 2 shows the activity zone of the inverted pendulum within which control can be achieved.

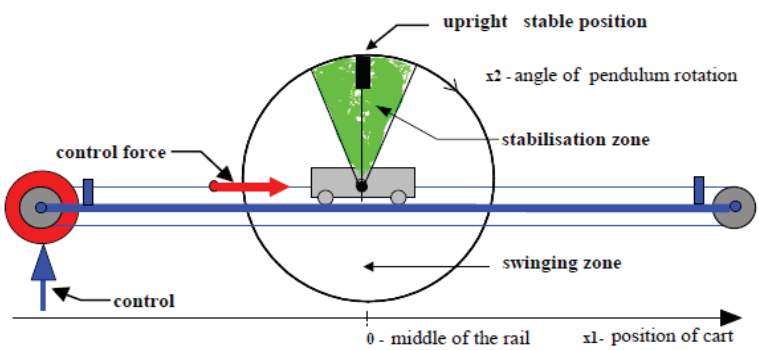


Figure 2. Activity zone of the control algorithm

### 2.1.1 System Modelling

The system schematics diagram is shown in Figure 3, with $\theta$, $x$, and $f(t)$ as pendulum angle, the cart displacement and applied force in ($N$) respectively. M is the mass of the cart ($kg$), $l$ is the pendulum length ($m$), and $I$ is the moment of inertia of the rod from the centre of mass ($kgm^2$). $C$ and $b$ are the translation and viscous damping of the cart ($Ns/m$) and that of the pendulum ($Nm/rad$) respectively (Zhang and Tu, 2006).

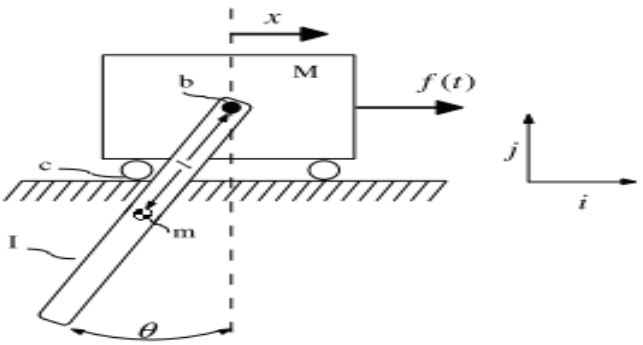


Figure 3. Schematic diagram of the pendulum-cart system

The energy in the system is simply its kinetic energy and potential energy. The total kinetic energy of the system can be expressed as in Equation (1);

$$T = T_M + T_m \tag{1}$$

where $T$ is the total kinetic energy, $T_M$ is the kinetic energy of the cart and $T_m$ is the kinetic energy of the pendulum, as expressed in Equations (2) to (3) as follows:-

$$T_M = \frac{1}{2} M \dot{x}^2 \tag{2}$$

$$T_m = \frac{1}{2} m V^2 + \frac{1}{2} I \omega^2 \tag{3}$$

where $V$ is the velocity of the pendulum's centre of mass and $I$ is the moment of inertia of the pendulum around the centre of mass and $\omega$ is the angular velocity of the pendulum. Also, the position vector can be given as in Equation (4) below:-

$$r = (x + l\sin\theta)\hat{i} + l\cos\theta\hat{j} \tag{4}$$

And the velocity vector can be express as given in Equation (5) below:-

$$V = \frac{dr}{dt} = \left(\dot{x} + lcos\theta\dot{\theta}\right)\hat{i} + lsin\theta\dot{\theta}\hat{j} \tag{5}$$

Putting $\omega = \dot{\theta}$, the kinetic energy of the pendulum is given as in Equation (6) below:-

$$T_m = \frac{1}{2}m(\dot{x}^2 + 2\dot{x}lcos\theta\dot{\theta} + l^2cos^2\theta\dot{\theta}^2 + l^2sin^2\theta\dot{\theta}^2) + \frac{1}{2}I\dot{\theta}^2 \tag{6}$$

Hence, the total kinetic energy of the system is as given in Equation (7) as follow:-

$$T = T_M + T_m = \frac{1}{2}M\dot{x}^2 + \frac{1}{2}m(\dot{x}^2 + 2\dot{x}lcos\theta\dot{\theta} + l^2cos^2\theta\dot{\theta}^2 + l^2sin^2\theta\dot{\theta}^2) + \frac{1}{2}I\dot{\theta}^2 \tag{7}$$

In addition, the total potential energy of the system is given as in Equation (8) below:-

$$V = V_M + V_m \tag{8}$$

where $V_M$ is the potential energy of the cart and $V_m$ is the potential energy of the pendulum. But, $V_M$ = 0, and the term $V_m$ is given as in the expression in Equation (9) below:-

$$V_m = mglcos\theta \tag{9}$$

Therefore, the total potential energy can be written as in Equation (10) below:-

$$V = V_M + V_m = mglcos\theta \tag{10}$$

The system dynamics equation of motion can be derive using Lagrange's equation as written in Equation (11) by Mishra and Chandra (2014) below:-

$$\frac{d}{dt}\left(\frac{\partial L}{\partial \dot{x}}\right) - \frac{\partial L}{\partial x} = \Xi_x \tag{11}$$

where, (L) is expressed in form of kinetic energy and potential energy of the system given in Equation (12) below:-

$$L = T - V \tag{12}$$

Substituting $T$ and $V$ in Equation (12), it is obtained as in Equation (13) below:-

$$L = \frac{1}{2}M\dot{x}^2 + \frac{1}{2}m\left(\dot{x}^2 + 2\dot{x}lcos\theta\dot{\theta} + l^2cos^2\theta\dot{\theta}^2 + l^2sin^2\theta\dot{\theta}^2\right) + \frac{1}{2}I\dot{\theta}^2 - mglcos\theta \quad (13)$$

Substituting Equation (13) into (11) and solving for the partial derivatives yields an expression in Equation (14) below:-

$$\frac{d}{dt}(M\dot{x} + m\dot{x} + mlcos\theta\dot{\theta}) = f(t) - c\dot{x} \quad (14)$$

The above equation can be represented as in the expression in Equation (15) below:-

$$(M + m)\ddot{x} + mlcos\theta\ddot{\theta} + mlsin\theta\dot{\theta}^2 + c\dot{x} = f(t) \quad (15)$$

Moreover, $\theta$ is given as in Equation (16) below:-

$$\frac{d}{dt}\left(\frac{\partial L}{\partial \dot{\theta}}\right) - \frac{\partial L}{\partial \theta} = \Xi_\theta \quad (16)$$

Substituting Equation (13) into (16) and solve for the partial derivatives yields an expression in Equation (17) as follows:-

$$\frac{d}{dt}\left(ml\dot{x}cos\theta + ml^2\dot{\theta} + I\dot{\theta}\right) + ml\dot{x}sin\theta\dot{\theta} + mglsin\theta = -b\dot{\theta} \quad (17)$$

Also, Equation (17) can be further simplified as given in Equation (18) below:-

$$(ml^2 + I)\ddot{\theta} + ml\ddot{x}cos\theta\dot{\theta} - ml\dot{x}sin\theta\dot{\theta} + ml\dot{x}sin\theta\dot{\theta} + mglsin\theta + b\dot{\theta} = 0 \quad (18)$$

After re-arranging, the overall dynamic equations of the system were obtained as in Equation (19) below:-

$$\begin{cases} (M + m)\ddot{x} + c\dot{x} + mlcos\theta\ddot{\theta} + mlsin\theta\dot{\theta}^2 = f(t) \\ (ml^2 + I)\ddot{\theta} + ml\ddot{x}cos\theta + mglsin\theta + b\dot{\theta} = 0 \end{cases} \quad (19)$$

*2.1.1.1 Model linearization*

To linearize the nonlinear system, two points have to be considered for equilibrium points. The pendulum in the upright position (unstable, $\theta$ = 0) and pendulum in the downward position (stable, $\theta = \pi$). This can be achieved by Taylor's series approximation, for a small angle deviation around an equilibrium point $\theta_0$ as expressed in Equation (20 below:-

$$\theta = \theta_o + \varepsilon \tag{20}$$

Taylor's series first order approximation is given as in Equation (21) below:

$$f(\theta) \approx f(\theta_o) + \varepsilon \frac{df}{d\theta} \tag{21}$$

where $\varepsilon \approx \theta$, a small angle deviation from equilibrium and $\dot{\varepsilon}^2 \approx 0$, higher order neglected. Pendulum in upright position (unstable, $\theta = 0$). The following functions can be linearized as

$sin\theta \cong \theta,$
$cos\theta \cong 1,$
$\dot{\theta}^2 = 0$

Thus, substituting these into Equation (19), the motion equations are obtained as given in Equation (22) below:-

$$\begin{cases} (M+m)\ddot{x} + c\dot{x} + ml\ddot{\theta} = f(t) \\ (ml^2 + I)\ddot{\theta} + ml\ddot{x} + mgl\theta + b\dot{\theta} = 0 \end{cases} \tag{22}$$

Pendulum downward position (stable, $\theta = \pi$). The following functions can also be linearized as :-

$sin\theta \cong -\theta,$
$cos\theta \cong -1,$
$\dot{\theta}^2 = 0$

Thus, the motion equations are obtained as expressed in Equations (23) below:-

$$\begin{cases} (M+m)\ddot{x} + c\dot{x} - ml\ddot{\theta} = f(t) \\ (ml^2 + I)\ddot{\theta} - ml\ddot{x} - mgl\theta + b\dot{\theta} = 0 \end{cases} \tag{23}$$

Hence, the system equations are represented in state space form as given in Equations (24) and (25) as follow:-

$$\dot{x} = Ax + Bu \tag{24}$$

$$y = Cx \tag{25}$$

The states vector of the system can be assigned as in Equation (26) below:-

$$z = \begin{bmatrix} z_1 \\ z_2 \\ z_3 \\ z_4 \end{bmatrix} = \begin{bmatrix} \theta \\ \dot{\theta} \\ x \\ \dot{x} \end{bmatrix} \tag{26}$$

where, $\theta, \dot{\theta}, x \text{ and } \dot{x}$ are the pendulum angle, angular velocity, Cart displacement and velocity of the Cart respectably (Kizir et al, 2010). Hence the dynamics equations can be represented in state space form as given in Equations (27) and (28) below:-

$$\begin{bmatrix} \dot{z}_1 \\ \dot{z}_2 \\ \dot{z}_3 \\ \dot{z}_4 \end{bmatrix} = \begin{bmatrix} 0 & 1 & 0 & 0 \\ \frac{(M+m)gml}{q} & \frac{(M+m)b}{q} & 0 & \frac{-cml}{q} \\ 0 & 0 & 0 & 1 \\ \frac{(ml)^2 g}{q} & \frac{bml}{q} & 0 & \frac{-c(I+ml^2)}{q} \end{bmatrix} \begin{bmatrix} z_1 \\ z_2 \\ z_3 \\ z_4 \end{bmatrix} + \begin{bmatrix} 0 \\ \frac{mlg}{q} \\ 0 \\ \frac{(I+ml^2)}{q} \end{bmatrix} f \tag{27}$$

$$y = \begin{bmatrix} 1 & 0 & 0 & 0 \\ 0 & 0 & 1 & 0 \end{bmatrix} \begin{bmatrix} z_1 \\ z_2 \\ z_3 \\ z_4 \end{bmatrix} + \begin{bmatrix} 0 \\ 0 \end{bmatrix} f \tag{28}$$

## 3.0 FULL STATE FEEDBACK CONTROLLER DESIGN

In this section, LQR controller was designed and implemented on real time system. Controllability, observability and stability test was carried out before applying the controller.

### *3.1.1 Controllability Test*

The system is said to be controllable if an input to the plant can take all the states from a desired initial state to a desired final state in a final time interval, otherwise is uncontrollable. Table 1 show the system parameters. The controllability matrix is given as in Equation (29) below:-

$$M_c = [\mathrm{B} \quad \mathrm{AB} \quad \mathrm{A^2B} \quad \mathrm{A^3B}] \tag{29}$$

Table 1. System Parameters

| Parameter | Value |
|---|---|
| Mass of cart (M) | 2.4 kg |
| Mass of pole (m) | 0.23 kg |
| Length of pole (l) | 0.38 m |
| Moment of inertia of the pole (I) | 0.099 kg/m$^2$ |
| Coefficient of friction of cart (b) | 0.05 Ns/m |
| Damping coefficient of pendulum (d) | 0.005 Nms/rad |
| Gravity (g) | 9.8 m/s$^2$ |

For controllability, the rank ($M_c$) of the matrix must be equal to the number of states of the system. Using the MATLAB command, $M_c$ was obtained to be 4, hence, the system is controllable.

### *3.1.2 Observability Test*

If all states of a system can be determined from an observation of y(t) over a finite time interval, the system is completely observable otherwise is unobservable (Ogata, 1997). The observability matrix is given as in Equation (30):-

$$M_o = [C^T \quad A^T C^T \quad (A^T)^2 C^T \quad (A^T)^3 C^T] \tag{30}$$

For observability, the rank ($M_o$) of the matrix must be equal to the number of the outputs of the system. Using the MATLAB command, the $M_o$ was obtained as 4 hence the system is completely observable.

### 3.1.3 Stability Test

Inverted pendulum system is an unstable system, thus before applying any control algorithms there is need to test the stability of the system before and after control action so that the performance of the controller can be observed. Using the pole zero map shown in Figure 4, it can be observed that some poles of the system is in the right hand plant hence the system is unstable.

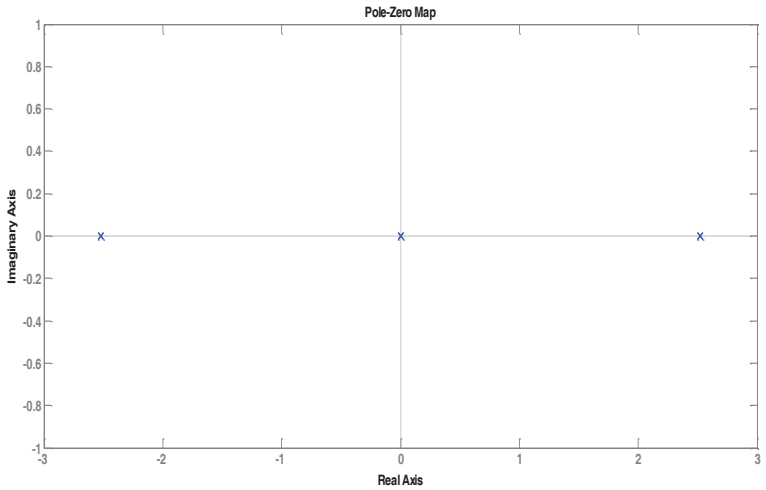


Figure 4. Poles and zero map of the open loop system

### 3.2 LQR Control Design

The LQR is a full state feedback controller that is usually used in industries for mechanical system control. The control of inverted pendulum using classical PID is mostly difficult because the system has higher state variables than the controller. Hence, as shown in Figure 5, a full state feedback controller is most suitable (Hauser and Saccon, 2005) and (Tahir et al, 2017).

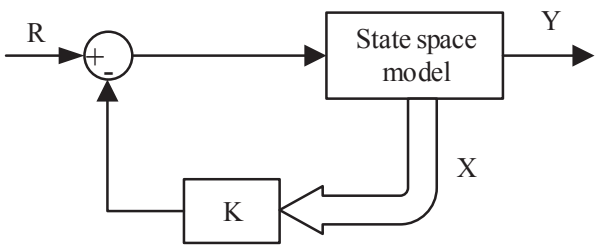


Figure 5. Typical LQR control system

In this control technique, a control law is selected $u = \psi(x)$ to regulate the state $x$ and minimize the performance index, as written in Equation (31):-

$$J = \int_0^\infty x^T(t)Qx(t) + u^T(t)Ru(t) \tag{31}$$

where J is the performance index function, $Q \geq 0 \; and \; R > 0$ are weight matrices for the state variable $x(t)$ and control variable $u(t)$ respectively. $Q$ and $R$ are the semi-positive definite matrix and positive definite matrix respectively (Ogata, 2010) and (Tahir et al, 2016). Thus, the gain vector K can be obtained to satisfy the feedback control law given as in (Tahir et al, 2017).

Moreover, the control variable can be expressed as in Equation (32) below:-

$$u = -Kx = -R^{-1}B^{T}Px \tag{32}$$

where $P$ is the solution of the Riccati equation given as in Equation (33) as follow:-

$$A^{T}P + PA + Q - PBR^{-1}B^{T}P = 0 \tag{33}$$

In which, the gain factor, $K$ is expressed in Equation (34) as below:-

$$K = R^{-1}B^{T}P \tag{34}$$

Bryson's rule states that *a* first choice of matrices $Q$ and $R$ is to select the matrices diagonals given as shown in Equations (35) and (36) below:-

$$Q_{ii} = \frac{1}{\text{maximum acceptable value of} X_i^2} \qquad i \in \{1,2,3,\ldots l\} \tag{35}$$

$$R_{jj} = \frac{1}{\text{maximum acceptable value of} u_j^2} \qquad j \in \{1,2,3,\ldots l\} \tag{36}$$

where $X_i$ and $u_i$ are the maximum expected value of the state and that of control signal respectively (Lingyan et al, 2009). Therefore, $Q$ and $R$ parameters were used in the following forms, as given in Equation (37) below:-

$$Q = \begin{bmatrix} Q_{11} & 0 & 0 & 0 \\ 0 & Q_{22} & 0 & 0 \\ 0 & 0 & Q_{33} & 0 \\ 0 & 0 & 0 & Q_{44} \end{bmatrix} \tag{37}$$

While, R can be expressed as in Equation (38) below:-

$$R = R_1 \tag{38}$$

The cart is constrained to lie between $-0.5 \leq x(t) \leq 0.5(m)$ and the input to the motor is constrained to lie between $-2.5 \leq u(t) \leq 2.5\ (v)$. Thus, $Q_{11} = \frac{1}{0.2^2} = 25$, is the weight due to angle, assuming a 0.2 rad maximum deviation expected from the upright position. $Q_{33} = \frac{1}{0.2^2} = 25$, is the weight due to the position of the cart and was assume that the cart should not exceed 0.2m from the centre of the rail. $R_1 = \frac{1}{2.5^2} = 0.16$, is the weight due to the control voltage. The close loop controller gain for both simulation and experiment were obtained as K = [58.2411 22.8208 -12.5000 -12.2993] and K = [44.72 200.8 -49.77 -27.38] respectably.

## 4.0 RESULTS AND DISCUSSION

The real time optimal control implementation of an inverted pendulum was presented. LQR was designed and implemented for swing up and stabilization control of an inverted pendulum. A Gaussian distributed noise and wind disturbance of magnitude 0.2 N was used to test the robustness of the control algorithms in both simulations and experiments respectively..

### 4.1 Simulation Results

The system is completely stable after applying the controller. Figure 6 shows the poles zeros map of the system, with details of the poles, damping, frequency, and overshoot of the system.

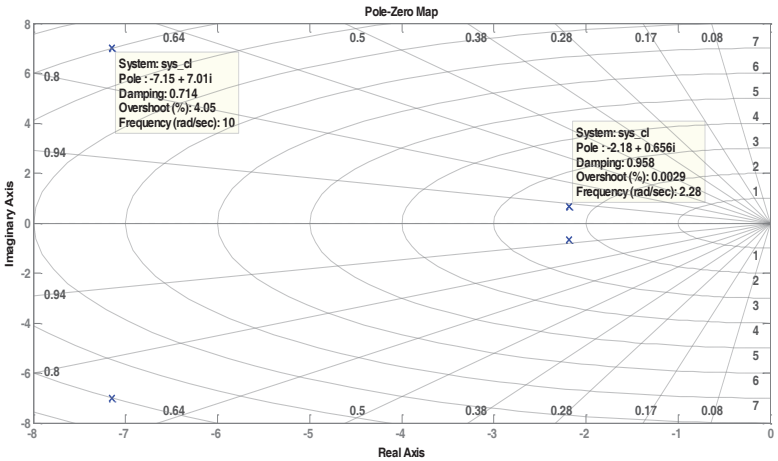


Figure 6. Closed loop poles-zeros map

The cart position, swing angle and control signal of the system were as shown in Figure 7, simulated with an initial condition of 0.1rad. The systems stabilized at 2 sec with 0.262 m undershoot of cart position and 0.08 m of the swing angle.

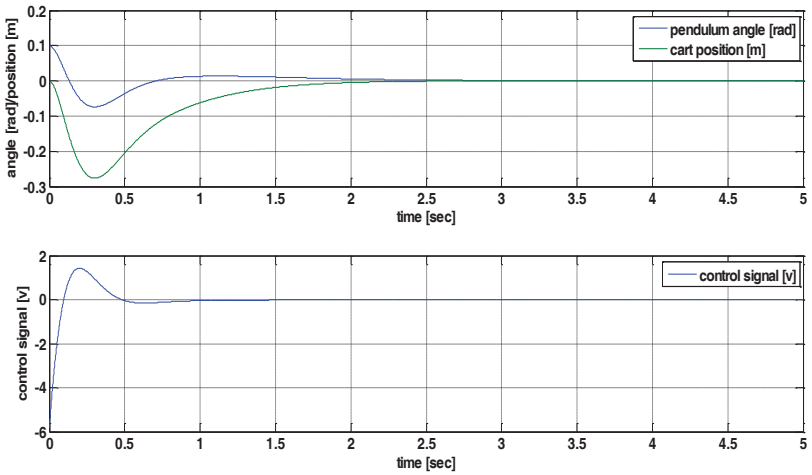


Figure 7. LQR control action of the system

In simulation, a Gaussian distributed noise of mean = 0.0001 and variance = 0.00001 was injected into the control system, at a sampling time of 0.5sec. As shown in Figure 8, the performance of the controller remained the same however, some negligible amplitude and frequency variations can be observed in the system.

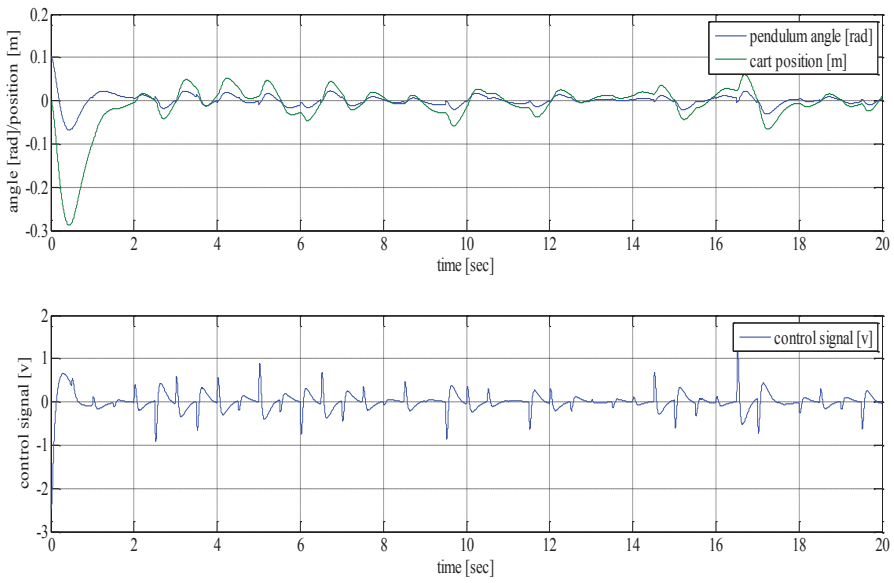


Figure 8. Disturbance injection response of the system with LQR

### *4.1.1 Experimental Results*

The experiment was conducted at simulation and control laboratory Glasgow Caledonian University UK. Figures 9 and 10 showed the photos of the real time experiment with swing up and stabilizing controller respectably, using the feedback instruments laboratory scale inverted pendulum system.

The algorithm was implemented in real time, the control signal, swing angle, and cart position is as shown in Figure 11, in which the pendula swing up and stabilized within the constraints voltage. It was observed that the controller shows a very good performance as it stabilized the system within the stabilization zone of 0.2 m. A good stabilization and swing up control was also achieved as in Figure 12, with the control action only starting at 13 sec. This is also within the stabilization zone of the system.

In addition, the experiment was conducted under a wind disturbance magnitude of 0.2 N and a very good performance was also achieved as shown in Figure 13 but from the control signal it can be observed that under disturbance, more voltage was consumed.

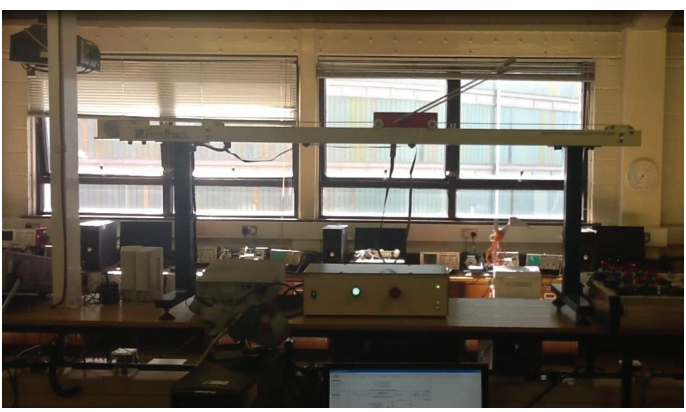

Figure 9. Pendulum in swing-up mode by swinging controller

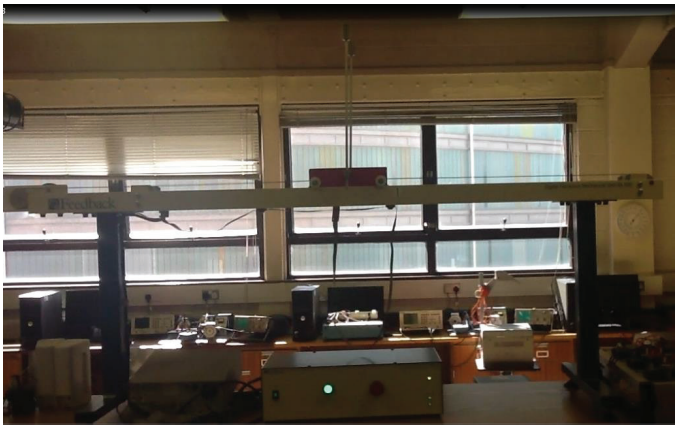

Figure 10. Pendulum in an upright position controlled by stabilizing controller

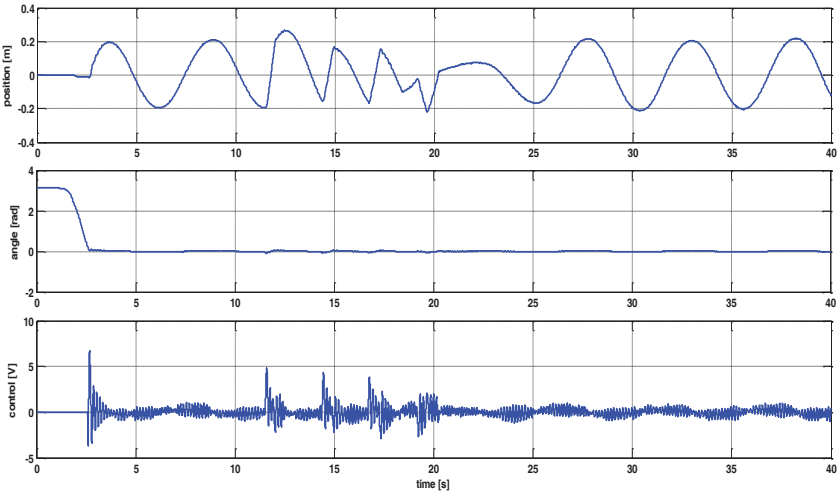


Figure 11. LQR stabilizing action experimental results

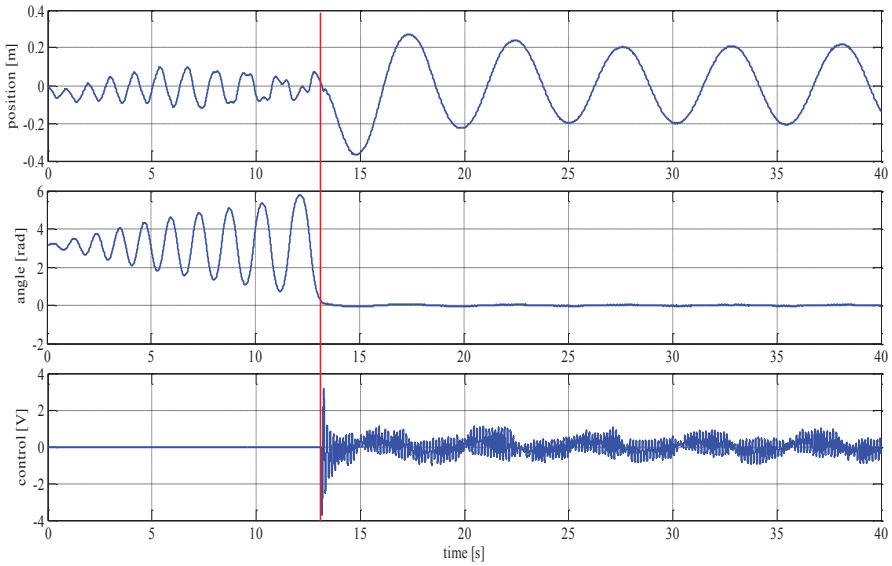


Figure 12. LQR Swing-up/stabilizing action experimental results

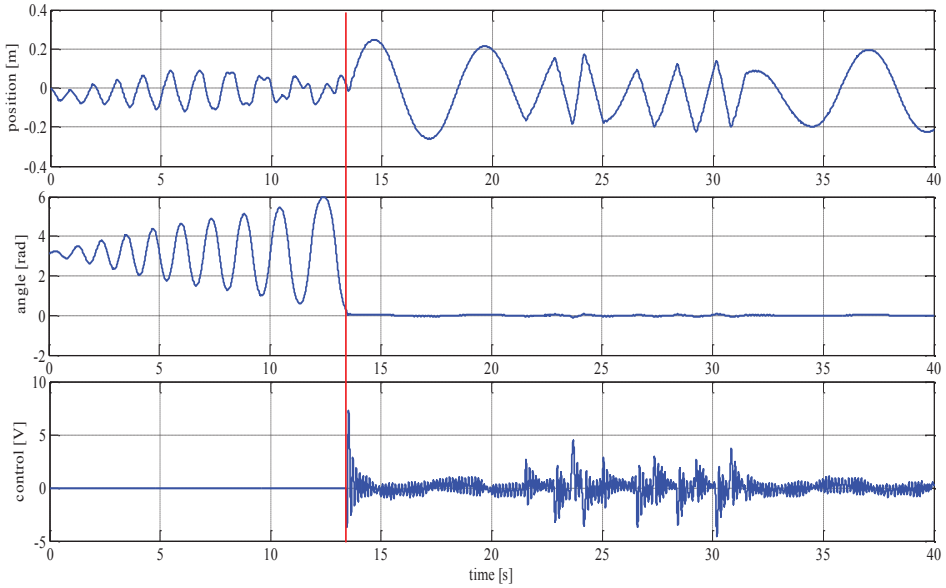


Figure 13. LQR Swing-up/stabilizing action experimental results under wind disturbance

## 5.0 CONCLUSION

In this paper, nonlinear inverted pendulum was linearized using Taylor series approach and LQR controller was designed to swing up and stabilize the pendulam. It was also implemented on real time system under wind disturbance. Time response specification and level of disturbances rejection were used as the performance index. Based on Simulation and experimental results, a very good performance was achieved and the controller is robust to external disturbances. To further reduce the oscillations amplitude and frequencies, enhance and improve the modelling and control for real time accuracies, frictional coefficients should be taking into consideration.

## ACKNOWLEDGEMENT

The authors are grateful to Glasgow Caledonian University, Scotland UK and Abubakar Tafawa Balewa University (ATBU) Bauchi, Nigeria for providing financial support and research resources.

## REFERENCES

Al-hadithi, B. M. (2012). Fuzzy Optimal Control for Double Inverted Pendulum. *7th IEEE Conference on Industrial Electronics and Applications. Singapore*, 1-5.

Bhangal, N. S. (2013). Design and Performance of LQR and LQR based Fuzzy Controller for Double Inverted Pendulum System. *Journal of Image and Graphics* 1(3): 143–146.

Brisilla, R. M. & Sankaranarayanan, V. (2015). Nonlinear control of mobile inverted pendulum. *Robotics. Autonomous. Syst.*, 70: 145–155.

Chakraborty, K., Mukherjee, R. R., and Mukherjee, S. (2013). Tuning of PID Controller of Inverted Pendulum Using Genetic Algorithm. *International Journal of Electronics and Communication Technologies,* 4(1): 183–186.

Chalupa, P. (2008). Modelling and Predictive Control of Inverted Pendulum. *Proceedings 22nd European Conference on Modelling and Simulation* ISBN: 978-0-9553018-5-8.

Chalupa, P., and Bobal, V. (2008). Modelling and Predictive Control of Inverted Pendulum. Proc. *22nd European Conf. Modelling Simulation*, 531–537.

Gupta, M. K. (2014). Stabilization of Triple Link Inverted Pendulum system based on LQR control Technique, *Recent Advances and Innovations in Engineering*.

Hauser, J. F. and Saccon, A. (2005). On the Driven Inverted Pendulum, Proceedings the *5th International Conference on Information, Communications and Signal Processing*, Bangkok.

Kizir, S., Bingul, Z. and Oysu, C., (2010). Fuzzy control of a real time inverted pendulum system. *Journal of Intelligent and Fuzzy Systems,* 21(1-2): 121-133.

Ogata, K. (2010). Modern Control Engineering. 5th edition, New Jersy: Prentice Hall.

Lingyan, H., Guoping L., Xiaoping L., and Zhang H, (2009). ThKumar, E. V. and Jerome, J.(2013) Robust LQR Controller Design for Stabilizing and Trajectory Tracking of Inverted Pendulum, *Procedia Eng,* 64:169–178.

Kumar, P., Mehrotra, O. N., and Mahto, J. (2012). Controller Design of Inverted Pendulum Using Pole Placement and Lqr, *International Journal of Research in Engineering and Technology* 532–538.

Mishra S. K., and Chandra, D. (2014). Stabilization and Tracking Control of Inverted Pendulum Using Fractional Order PID Controllers. *Journal of Engineering*, 1-9.

Mus N. and Tovornik B. (2006). Swinging Up and Stabilization of a Real Inverted Pendulum, *IEEE Transactions on Industrial Electronics,* 53(2): 631–639.

Prasad, L. B.(2014). Optimal Control of Nonlinear Inverted Pendulum System Using PID Controller and LQR : *IEEE International Conference on Control System, Computing and Engineering*, 11: 661–670.

Riachy S.,Orlov, Y., Floquet, T., Santiesteban R., and Richard. J. (2007). Second-order Sliding Mode Control of Under Actuated Mechanical Systems I: Local Stabilization with Application to an Inverted Pendulum. *International Journal of Robust and Nonlinear Control*, 18(4-5). 529-54.

Shamsudin, M. A., Mamat, R., and Nawawi, S. W. (2013). Dynamic Modelling and Optimal Control Scheme Of Wheel Inverted Pendulum for Mobile Robot Application, *International Journal of Control Theory and Computer Modelling*, 3(6): –20.

Singh, K., Nema, S. and Padhy, P. K. (2014). Modified PSO based PID Sliding Mode Control for Inverted Pendulum, *International Conference on Control, Instrumentation, Communication and Computational Technologies*, 722–727.

Singh N. and Yadav, S. K. (2012). Comparison of LQR and PD controller for stabilizing Double Inverted Pendulum System, *International Journal of Engineering Research and Development*. ISSN: 2278-067X, 1(12): 69-74.

Tijani, I. B. (2013). Control of an inverted pendulum using MODE-based Optimized LQR controller, *IEEE Conference on Industrial Electronics and Applications*, 1759–1764.

Tahir, N.M, Hassan,S.M, Mohamed, Z. and Ibrahim,A.G. (2017). Output based Input Shaping for Optimal Control of Single Link Flexible Manipulator, *International Journal on Smart Sensing and Intelligent Systems*, 10(2): 367-386.

Tahir,N.M, Bature, A.A, Bature U. I, Sambo A. U, and Babawuro A.Y. (2016). Vibration and Tracking Control of A Single Link Flexible Manipulator Using LQR and Command Shaping. *Journal of Multidisciplinary Engineering Science and Technolog,* ISSN: 2458-9403. 3(3).

Yang, C., Li, Z., Member, S., and Cui, R., (2014). Neural Network-Based Motion Control of Underactuated Wheeled Inverted Pendulum Models. *IEEE Transactions on Neural Networks and Learning Systems*. 25(11).

Zhang L., and Tu, Y. (2006) Research of Car Inverted Pendulum Model Based on Lagrange Equation. *The Sixth World Congress on Intelligent Control and Automation*, 820-824.